EPJ Web of Conferences **270**, 00019 (2022) https://doi.org/10.1051/epjconf/202227000019
QCD@Work 2022

A journey through the experimental highlights on heavy-ion physics

Alberto Calivà[1,2,*]

[1]University of Salerno, Physics Department "E.R. Caianiello", via Giovanni Paolo II, 132 84084 Fisciano, Italy
[2]National Institute for Nuclear Physics (INFN), Section of Napoli, group of Salerno, via Giovanni Paolo II, 132 84084 Fisciano, Italy

Abstract. Heavy-ion collisions are a unique tool to create in the laboratory the quark-gluon plasma (QGP), a state of strongly-interacting matter where quarks and gluons are deconfined. Significant progress was made over the last years in the understanding of the QGP properties and in the characterization of the phase diagram of QCD matter. In these proceedings, a review of recent experimental highlights on heavy-ion physics from different experiments is presented.

1 Introduction

One of the main goals of studying heavy-ion collisions is to characterize the properties of the quark-gluon plasma (QGP), a deconfined phase of quarks and gluons, and explore the phase diagram of QCD matter. The latter is a two-dimensional space where a state of QCD matter is defined by its temperature and baryochemical potential μ_B. Different regions of the phase diagram can be accessed with heavy-ion collisions at different center-of-mass energies. The space-time evolution of heavy-ion collisions comprises several stages that can be studied using different experimental probes and methods. The overall picture, containing the current knowledge of the QPG properties and of the phase diagram, emerges from a complex and diverse experimental program involving many experiments at different facilities running at center-of-mass energies per nucleon pair covering the range from a few GeV to TeV. In the following, a review of selected highlights on heavy-ion physics from different experiments is presented and the interpretation of the results is discussed.

1.1 Heavy Quarkonia

Quarkonia are flavorless mesons made of heavy quark-antiquark pairs. Charm and bottom quarks are created in the early stages of the collision in hard parton-parton scattering processes. These particles then travel through the hot and dense QCD medium losing a fraction of their energy before hadronization in collisions with other partons and (mostly) by gluon radiation. The energy loss effects can be quantified by the nuclear modification factor R_{AA}, defined as the ratio of the measured quarkonium yield in heavy-ion collisions and the $\langle N_{coll} \rangle$-scaled yield measured in pp collisions at the same energy, where $\langle N_{coll} \rangle$ is the average number

*e-mail: alberto.caliva@cern.ch

of binary nucleon-nucleon collisions. The R_{AA} of inclusive J/ψ at mid-rapidity was measured both at RHIC and LHC energies, as shown in Fig. 1. The R_{AA} continuously decreases with increasing average number of participant nucleons ($\langle N_{\rm part}\rangle$) at RHIC energy [1, 2] while and enhancement is observed at LHC energy starting from $\langle N_{\rm part}\rangle \approx 100$. This effect is due to the recombination of charm-anticharm pairs in the late stages of the QGP evolution close to the phase boundary, as predicted by different theoretical works several years ago [3–6]. Recombination effects, which become stronger going to more central collisions and lower transverse momentum ($p_{\rm T}$), are observed also for the $\psi(2S)$.

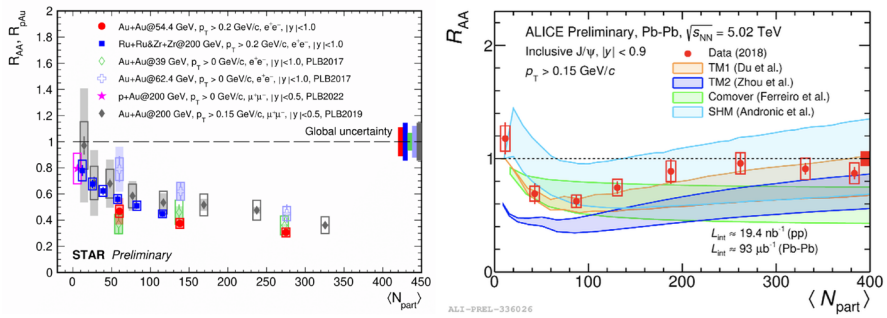

Figure 1. R_{AA} of inclusive J/ψ at mid-rapidity measured at RHIC (left) and LHC (right) energies as a function of the average number of participant nucleons ($\langle N_{\rm part}\rangle$).

The elliptic flow (v_2), i.e. the second coefficient in the Fourier expansion of azimuthal particle distribution with respect to the symmetry plane of the collision, is also sensitive to recombination effects and can be used to further characterize the J/ψ production mechanism. While the v_2 of inclusive J/ψ measured in Au–Au collisions at $\sqrt{s_{\rm NN}} = 200$ GeV at RHIC is consistent with zero, both prompt and non-prompt J/ψ show a significant v_2 up to high $p_{\rm T}$, as measured by CMS. These results confirm the absence of significant $c\bar{c}$ recombination effects and early production of charmonia at RHIC energies. On the contrary, the large v_2 of prompt and non-prompt J/ψ measured at the LHC at low p_T implies a high degree of thermalization of charm quarks and a significant contribution from regeneration.

Since the $c\bar{c}$ recombination occurs in the late stages of the collision, the v_2 of different quarkonium states is sensitive to the time when their regeneration happens. Indeed, the v_2 of the prompt $\psi(2S)$ measured by CMS is larger than that of the prompt J/ψ, which could be explained by a sequential regeneration of charmonia [7]. Another interesting effect predicted many years ago and considered a decisive signature of the QGP formation [8] is the sequential suppression of higher-mass quarkonium states. Evidence of this effect is found not only for charmonium but also for bottomonium states, as recently shown by both ATLAS and CMS Collaborations.

1.2 Open Heavy Flavor

Open heavy-flavor hadrons are complementary probes to charmonia to study the in-medium energy loss of heavy quarks and characterize the QGP properties. Since the bottom quark is heavier than charm, it is expected to lose a lower fraction of its energy in collisions with other partons and by gluon radiation (dead cone effect). This is confirmed by the measurement of the R_{AA} of electrons from charm and bottom decays in central Au–Au collisions at $\sqrt{s_{\rm NN}} =$

200 GeV by PHENIX and also by the measurement of prompt and non-prompt D mesons by ALICE [9]. The R_{AA} and v_2 of prompt D mesons are used by ALICE to constrain the spatial diffusion coefficients of charm. Interestingly, charm and bottom quarks are also sensitive to initial state fluctuations in the spatial distribution of nucleons participating in the collision for a given impact parameter. This is demonstrated by the significant v_3 of prompt and non-prompt D^0 mesons measured by CMS in mid-central Pb–Pb collisions at $\sqrt{s_{NN}}$ = 5.02 TeV as shown in Fig 2. The bottom quark is less sensitive than charm due to its larger mass.

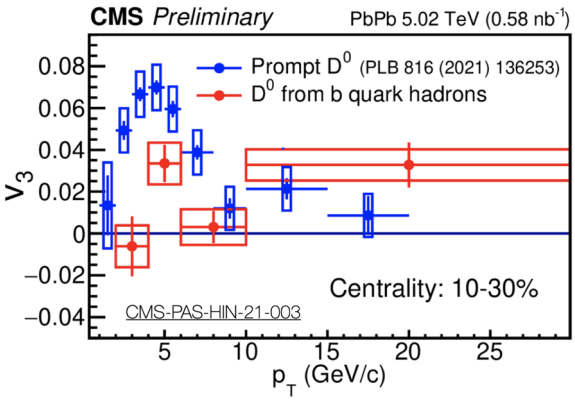

Figure 2. v_3 of prompt and non-prompt D^0 mesons measured by CMS in Pb–Pb collisions at $\sqrt{s_{NN}}$ = 5.02 TeV.

1.3 Light Flavor

In the light-flavor sector, one of the most debated topics is the production mechanism of light (anti)nuclei in high-energy hadronic collisions. The statistical hadronization model [10–16] and nucleon coalescence [17–23] are the main competing models that are based on different microscopic processes. Both models provide similar predictions of (anti)nuclei yields, therefore novel techniques and observables have recently been introduced to distinguish these (anti)nucleosynthesis models. One of them is the (anti)nuclei number fluctuation. The STAR Collaboration has recently reported the first measurement of the deuteron-deuteron femtoscopic correlation function in Au–Au collisions at $\sqrt{s_{NN}}$ = 3 GeV and the center-of-mass energy dependence of the proton-deuteron Pearson coefficient, as illustrated in Fig 3. Both measurements are consistent with model calculations incorporating nucleon coalescence, while the Pearson coefficient measurement is also compatible with the canonical statistical hadronization model [16, 24].

The (anti)deuteron number fluctuation has been recently measured also by the ALICE Collaboration [25]. The cumulant ratio $\kappa_2/\kappa_1 = \langle(n_d - \langle n_d\rangle)^2\rangle/\langle n_d\rangle$, where n_d is the measured number of deuterons per event, and the proton-deuteron Pearson correlation coefficient favor the canonical statistical model over the coalescence approach. Interestingly, this measurement indicates a smaller correlation volume, i.e. the volume in which the baryon number conservation is implemented, with respect to the net-proton fluctuation measurement [26].

The above-mentioned (anti)nucleosynthesis models describe also the production of exotic hypernuclei, i.e. nuclei with hyperons. The hypertriton ($^3_\Lambda$H) yields measured by STAR in Au–Au collisions at $\sqrt{s_{NN}}$ = 3, 19.6 and 27 GeV and the first measurement of

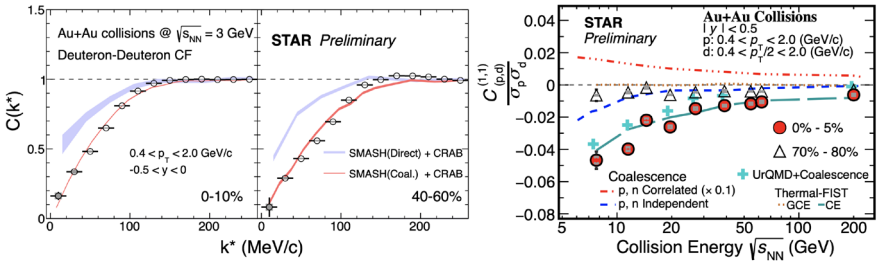

Figure 3. Deuteron-deuteron correlation function measured in Au–Au collisions at $\sqrt{s_{\rm NN}} = 3$ GeV (left) and the center-of-mass energy dependence of the proton-deuteron Pearson coefficient (right) measured by STAR.

the hyperhydrogen-4 ($^4_\Lambda$H) in Au–Au collisions at $\sqrt{s_{\rm NN}} = 3$ GeV, shown in Fig 4, are essential to constrain the production models at high $\mu_{\rm B}$. Also in this case, the coalescence approach provides a good description of the data while some configurations of SHM and hybrid models fail.

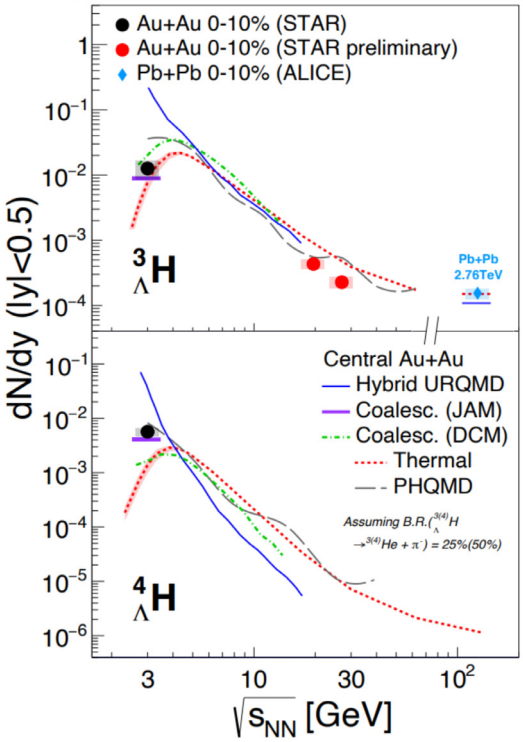

Figure 4. Hypernuclei yields measured by STAR in Au–Au collisions at $\sqrt{s_{\rm NN}} = 3$, 19.6 and 27 GeV in comparison with hypernuclei production models.

In the coalescence approach, the production yield of the hypertriton depends on the radial extension of its wave function. Recent measurements of the hypertriton lifetime, performed by different experiments, consistently yield a value that is very close to that of the free Λ. These results confirm that the hypertriton is a loosely bound object, thus closing the long-standing hypertriton lifetime puzzle [27].

The properties of the hadron gas phase, produced after hadronization, can be studied by measuring the yields of short-lived resonances. Due to their short lifetimes, which are comparable to that of the hadron gas phase, resonance yields are affected by re-scattering effects of their decay daughters with other hadrons in the gas and also by re-generation effects, i.e. the back reaction to their decay. The STAR Collaboration has reported measurements of the yield ratios K^{*0}/K and Φ/K as a function of multiplicity. A significant decrease is observed for K^{*0}/K with increasing multiplicity, while the ratio Φ/K is almost flat. This is due to the competing strangeness enhancement effect i.e. the increase in the ratio of strange to non-strange hadron yields with increasing multiplicity [28]. To further characterize the hadron gas phase, the ALICE Collaboration has measured the yield ratios of resonances with different lifetimes to those of the corresponding stable hadrons. Figure 5 shows the $K^{*\pm}/K^0_S$ and $\Lambda(1520)/\Lambda$ measured as a function of multiplicity in different collision systems and center-of-mass energies. Although the $\Lambda(1520)$ has a longer lifetime than K^*, it shows a stronger suppression when going from peripheral to central Pb–Pb collisions. Obviously, the lifetime is not a good predictor for resonance suppression, which depends on the mean free path of the resonance in the hadron gas phase and on the (partial) chemical equilibrium with the system [29].

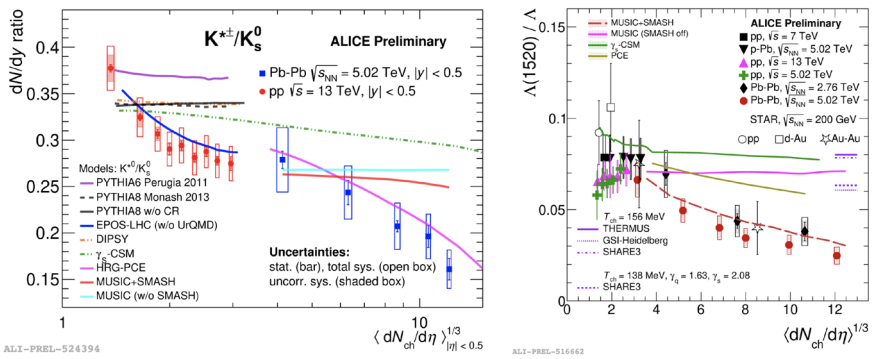

Figure 5. $K^{*\pm}/K^0_S$ and $\Lambda(1520)/\Lambda$ measured by ALICE as a function of multiplicity in different collision systems and center-of-mass energies.

1.4 Direct Photons and Dileptons

Direct photons and dileptons, i.e. lepton-antilepton pairs from virtual photons, are electromagnetic probes that are emitted continuously throughout the entire history of a heavy-ion collision. These particles interact with the medium only through the electroweak force, hence they carry undisturbed information on the production process. The PHENIX Collaboration has recently reported the measurement of non-prompt direct-photon production in Au–Au collisions at $\sqrt{s_{\rm NN}}$ = 200 GeV [30]. The non-prompt direct-photon $p_{\rm T}$ spectrum is obtained by subtracting from the inclusive direct-photon spectrum measured in Au–Au collisions the prompt component, estimated using the $\langle N_{\rm coll}\rangle$-scaled direct-photon spectrum measured in pp

collisions at the same energy. The extracted non-prompt direct-photon spectrum is consistent with theoretical calculations including pre-equilibrium and thermal photons at high p_{T}, while at low p_{T}, there is a hint of an excess of non-prompt direct-photon production with respect to the expectations both in central and peripheral collisions. The inverse slope parameter $\langle T_{\mathrm{eff}} \rangle$, extracted from an exponential fit to the non-prompt direct-photon spectrum, is studied as a function of p_{T} and multiplicity. A higher effective average temperature is observed for higher p_{T}, with no significant multiplicity dependence. This implies that different p_{T} regions of the spectrum are sensitive to different stages of the collision and that $\langle N_{\mathrm{coll}} \rangle$-scaling of direct-photon production holds approximately within the multiplicity interval covered by the measurement.

The inverse slope parameter of the direct-photon spectrum is affected by blue shift due to radial flow. Instead, the temperature extracted from a fit to the invariant-mass excess spectrum of dileptons in the mass region $m_{\phi} < m_{ll} < m_{J/\psi}$, dominated by thermal radiation from QGP, is not influenced by radial flow. The excess dilepton spectrum is obtained by subtracting from the inclusive spectrum the contribution from hadron decays, the so-called "hadronic cocktail". The latter is obtained from simulations based on parametrized p_{T} distributions of hadrons from data and scaling laws obtain the input distributions of hadrons that are not measured. The dilepton excess spectrum was measured by STAR in Au–Au collisions at $\sqrt{s_{\mathrm{NN}}}$ = 27 and 54.4 GeV and compared with previous results in In–In collisions at $\sqrt{s_{\mathrm{NN}}}$ = 17.3 GeV at NA61, as shown in Fig. 6 left. Higher temperatures and yields are obtained at RHIC indicating a hotter and longer-lived QGP at RHIC than at the SPS. The excess spectrum is compared with theoretical model calculations including thermal radiation from the QGP and contributions from in-medium ρ^0 decays, characterized by a broader spectral function, as shown in Fig 6 right. A good agreement is found with different approaches in the mass region $0.2 < m_{ll} < 1.3$ GeV, while the model calculations underestimate the slope of the invariant-mass spectrum for $m_{ll} > m_{\phi}$, thus implying that the QGP is hotter than predicted in the models.

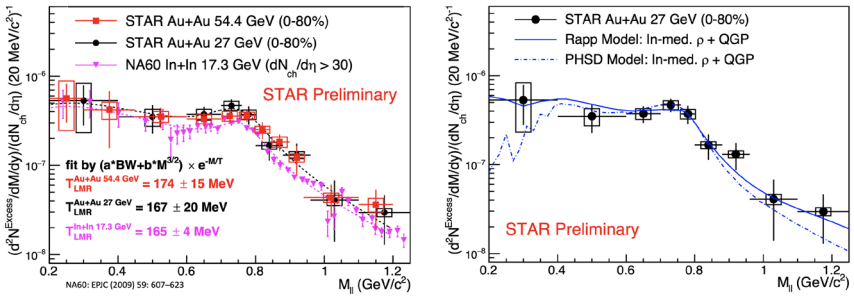

Figure 6. Dilepton excess spectra measured by STAR and NA61 at the SPS (left) and comparison with model calculations (right).

The first dilepton spectrum in Pb–Pb collisions at $\sqrt{s_{\mathrm{NN}}}$ = 5.02 TeV was measured by the ALICE Collaboration, as shown in Fig. 7 left. The measured spectrum is consistent with contributions from hadron decays, QGP radiation, and in-medium ρ^0 decays. Two different versions of the hadronic cocktail are compared to the data: one is based on $\langle N_{\mathrm{coll}} \rangle$-scaling of correlated semi-leptonic heavy-flavor decays, while in the other, heavy-flavor suppression is implemented by scaling the heavy-flavor contributions by the measured $R_{\mathrm{AA}}^{c/b \to e}$ [31]. The lat-

ter version of the cocktail gives a better agreement with the data. The fraction of virtual direct photons is extracted from the low-mass region in different p_{T} intervals. This fraction is then scaled by the inclusive photon spectrum measured using the photon-conversion technique to obtain the first direct-photon spectrum at LHC. This is shown in Fig. 7 right in comparison with theoretical model calculations including prompt, pre-equilibrium, and thermal photons. All theoretical approaches give a good description of the measured spectrum considering the experimental uncertainties.

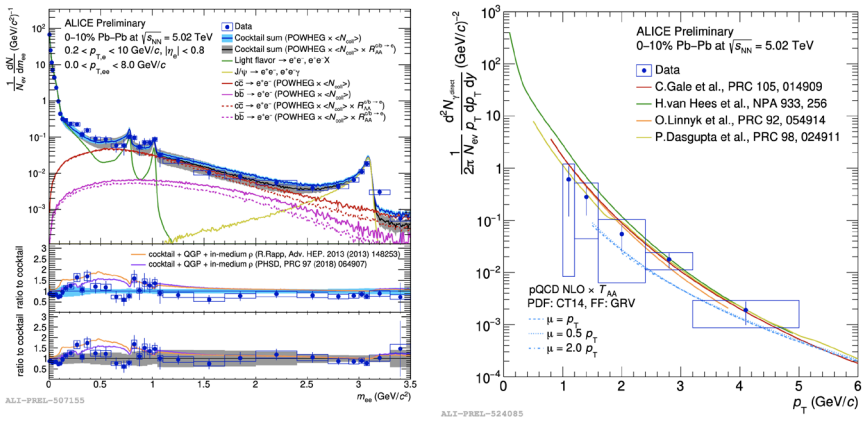

Figure 7. Dilepton spectrum measured in central Pb–Pb collisions at $\sqrt{s_{\mathrm{NN}}}$ = 5.02 TeV (left) and direct-photon spectrum (right).

2 Conclusions

Significant progress has been made over the last few years in the field of high-energy nuclear physics and hadronic physics at particle colliders. This includes a detailed characterization of the QGP properties and an in-depth understanding of a large variety of phenomena related to hadron production and hadronic interactions. The study of rare events and high-precision measurements at the TeV-energy scale will be possible with the restart of the LHC. Exciting times are ahead with the start of sPHENIX at RHIC and with future detectors and upgrades.

References

[1] L. Adamczyk et al., Phys. Lett. **B771**, 13 (2017)
[2] J. Adam et al., Phys. Lett. **B797**, 134917 (2019)
[3] B. Svetitsky, Phys. Rev. **D37**, 2484 (1988)
[4] P. Braun-Munzinger, J. Stachel, Phys. Lett. **B490**, 196 (2000)
[5] R.L. Thews, M. Schroedter, J. Rafelski, Phys. Rev. **C63**, 054905 (2001)
[6] A. Andronic et al., Phys. Lett. **B797**, 134836 (2019)
[7] X. Du, R. Rapp, Nucl. Phys. **A943**, 147 (2015)
[8] S. Digal, P. Petreczky, H. Satz, Phys. Rev. **D64**, 094015 (2001)
[9] S. Acharya et al. (ALICE Collaboration), J. High Energ. Phys. **174** (2022)
[10] J. Cleymans et al., Phys. Rev. **C84**, 054916 (2011), 1105.3719
[11] A. Andronic, others., Phys. Lett. **B697**, 203 (2011), 1010.2995
[12] F. Becattini et al., Phys. Rev. **C90**, 054907 (2014), 1405.0710
[13] V. Vovchenko, H. Stöcker, Phys. Rev. **C95**, 044904 (2017), 1606.06218
[14] A. Andronic et al., Nature **561**, 321 (2018), 1710.09425
[15] N. Sharma et al., Phys. Rev. **C99**, 044914 (2019), 1811.00399
[16] V. Vovchenko, B. Dönigus, H. Stoecker, Phys. Rev. **C100**, 054906 (2019), 1906.03145
[17] S.T. Butler, C.A. Pearson, Phys. Rev. **129**, 836 (1963)
[18] J.I. Kapusta, Phys. Rev. **C21**, 1301 (1980)
[19] R. Scheibl, U.W. Heinz, Phys. Rev. **C59**, 1585 (1999), nucl-th/9809092
[20] W. Zhao et al., Phys. Rev. **C98**, 054905 (2018), 1807.02813
[21] K. Blum, M. Takimoto, Phys. Rev. **C99**, 044913 (2019), 1901.07088
[22] K.J. Sun, C.M. Ko, B. Dönigus, Phys. Lett. **B792**, 132 (2019), 1812.05175
[23] M. Kachelrieß, S. Ostapchenko, J. Tjemsland, Eur. Phys. J. **A56**, 4 (2020), 1905.01192
[24] V. Vovchenko, B. Dönigus, H. Stoecker, Phys. Lett. **B785**, 171 (2018), 1808.05245
[25] ALICE Collaboration (2022), https://arxiv.org/abs/2204.10166
[26] ALICE Collaboration (2022), https://arxiv.org/abs/2206.03343
[27] A. Pérez-Obiol, D. Gazda, E. Friedman, A. Gal, Phys. Lett. **B811**, 135916 (2020)
[28] J. Adam et al., Nature Physics **13**, 535 (2017)
[29] A. Motornenko et al., Phys. Rev. **C102**, 024909 (2020)
[30] U.A. Acharya, others. (2022), https://arxiv.org/abs/2203.17187
[31] S. Acharya et al., J. High Energ. Phys. **2018** (2018)